

- GFP-VIVIT expression vector contained an oligonucleotide coding for MAGPHPVIVITGPHEE at the NH₂-terminus of GFP. Twenty-four hours after transfection, cells were stimulated for 6 hours with phorbol 12-myristate 13-acetate (PMA) (20 nM) and ionomycin (1 μM) or with immobilized anti-CD3 (0.2 μg/ml) (HIT3a, Pharmingen) and soluble anti-CD28 (0.5 μg/ml) (CD28.2, Pharmingen). CsA was added 30 min before the stimuli. Luciferase activity in cell lysates was normalized to levels of hGH.
12. The calcineurin targeting site of murine NFAT1, GPSPRIETPSHELMQAGG (residues 108 through 126) was mutated to GHPHPVIVITCPHELMQAGG (substitutions underlined) by replacing the DNA encoding the wild-type NFAT1 sequence between flanking Bsp 120I and Eco O109I sites with an oligonucleotide encoding the mutant sequence. Dephosphorylation of HA-NFAT1-GFP (9) was assessed in whole-cell extracts by protein immunoblotting, and subcellular localization was analyzed by GFP fluorescence (5).
 13. Jurkat cells cotransfected with murine CD4 (mCD4) (0.75 mg per 10⁶ cells) and GFP or GFP-VIVIT (0.75 μg per 10⁶ cells) were selected with magnetic beads coated with anti-mCD4 (Dynabeads L3T4, Dynal, Lake Success, NY) (22). The selected mCD4-expressing cells were >90% GFP- or GFP-VIVIT-positive, whereas mCD4-nonexpressing cells were <5% GFP-positive, as assessed by fluorescence microscopy. Multiprobe RNase protection assays were performed with the RiboQuant multiprobe kit (Pharmingen) (22).
 14. A. M. Ranger *et al.*, *Nature* **392**, 186 (1998); J. L. de la Pompa *et al.*, *ibid.*, p. 182.
 15. I.-C. Ho, J. H.-J. Kim, J. W. Rooney, B. M. Spiegelman, L. H. Glimcher, *Proc. Natl. Acad. Sci. U.S.A.* **95**, 15537 (1998).
 16. A. C. Greenlund *et al.*, *Immunity* **2**, 677 (1995); U. Schindler, P. Wu, M. Rothe, M. Brasseur, S. L. McKnight, *ibid.*, p. 689; T. Tsukazaki, T. A. Chiang, A. F. Davison, L. Attisano, J. L. Wrana, *Cell* **95**, 779 (1998); L. Attisano and J. L. Wrana, *Curr. Opin. Cell Biol.* **10**, 188 (1998); T. Kallunki, T. Deng, M. Hibi, M. Karin, *Cell* **87**, 929 (1996); A. J. Whitmarsh, J. Cavanagh, C. Tournier, J. Yasuda, R. J. Davis, *Science* **281**, 1671 (1998).
 17. N. H. Sigal *et al.*, *J. Exp. Med.* **173**, 619 (1991); M.

Pascual *et al.*, *Immunol. Today* **11**, 514 (1998). M. Hojo *et al.*, *Nature* **397**, 530 (1999); G. J. Nabel, *ibid.*, p. 471; M. J. Mihatsch *et al.*, *Clin. Nephrol.* **49**, 356 (1998); M. Cecka, *Surg. Clin. North. Am.* **78**, 133 (1998).

18. C. Loh *et al.*, *J. Biol. Chem.* **271**, 10884 (1996).
19. C. Luo *et al.*, *Mol. Cell. Biol.* **16**, 3955 (1996).
20. F. Mercurio *et al.*, *Science* **278**, 860 (1997).
21. J. P. Northrop *et al.*, *Nature* **369**, 497 (1994); T. Hoey, Y. L. Sun, K. Williamson, X. Xu, *Immunity* **2**, 461 (1995).
22. A. Kiani, J. P. B. Viola, A. H. Lichtman, A. Rao, *Immunity* **7**, 849 (1997).
23. We thank M. Berne for peptide synthesis and sequencing; D. Littman, G. Crabtree, and T. Hoey for reagents; and members of the laboratory for helpful discussion and advice. Supported by NIH grants R01 AI 40127 (to A.R.), R43 AI 43726 (to P.G.H.), R01 HL 03601 (to M.B.Y.), and R01 GM 56203 (to L.C.C.); by the Ministerio de Educación y Ciencia, Spain (C.L.-R.); and by the Arthritis Foundation (J.A.).

3 June 1999; accepted 24 August 1999

Identification of an RNA-Protein Bridge Spanning the Ribosomal Subunit Interface

Gloria M. Culver,* Jamie H. Cate,† G. Zh. Yusupova, Marat M. Yusupov, Harry F. Noller‡

The 7.8 angstrom crystal structure of the 70S ribosome reveals a discrete double-helical bridge (B4) that projects from the 50S subunit, making contact with the 30S subunit. Preliminary modeling studies localized its contact site, near the bottom of the platform, to the binding site for ribosomal protein S15. Directed hydroxyl radical probing from iron(II) tethered to S15 specifically cleaved nucleotides in the 715 loop of domain II of 23S ribosomal RNA, one of the known sites in 23S ribosomal RNA that are footprinted by the 30S subunit. Reconstitution studies show that protection of the 715 loop, but none of the other 30S-dependent protections, is correlated with the presence of S15 in the 30S subunit. The 715 loop is specifically protected by binding free S15 to 50S subunits. Moreover, the previously determined structure of a homologous stem-loop from U2 small nuclear RNA fits closely to the electron density of the bridge.

Ribosomes are large ribonucleoprotein complexes that are responsible for the fundamental process of protein synthesis. They are composed of two asymmetric subunits, each of which contributes to specific functions during translation. The interface between these subunits allows for the coordination of these discrete functions and also provides the binding surfaces for many substrates and ligands. Thus, the identification of specific molecular interactions between the two sub-

units is of great importance. Numerous experiments have identified RNA and protein elements that potentially contribute to this subunit-subunit interface (1–3). However, in the absence of high-resolution structural information, identification of the molecular components comprising specific subunit-subunit interactions has been difficult.

The 7.8 Å x-ray crystal structure of the *Thermus thermophilus* 70S ribosome (4) shows that the two ribosomal subunits are connected by a complex network of molecular interactions. One of these (bridge B4) can be identified as a double-stranded RNA stem-loop that is continuous with the 50S subunit and makes contact with the bottom of the platform of the 30S subunit (Fig. 1). Immunoelectron microscopy and preliminary modeling studies of the 30S subunit based on extensive biochemical, biophysical, and phylogenetic evidence localize the

binding site for protein S15 to this region of the 30S subunit (5). Additionally, evidence for the placement of S15 at the subunit interface has come from intersubunit cross-linking studies (2) and a temperature-sensitive S15 mutant that is defective in subunit association (6).

To test the possible proximity of S15 to 23S ribosomal RNA (rRNA), we performed directed hydroxyl radical probing (7). Iron(II) was tethered by a linker, 1-(*p*-bromoacetamidobenzyl)-EDTA (BABE) (8), to unique cysteine (C) residues on the surface of S15 at amino acid positions 12, 36, 46, and 70 by directed mutagenesis (9), using the published solution and crystal structures of S15 as a guide (10). The Fe(II)-derivatized proteins were incorporated into 30S subunits by in vitro reconstitution (11) and associated with 50S subunits to form 70S ribosomes, which were then purified by sucrose gradient centrifugation. The 30S subunits containing S15 derivatized at position 70 failed to associate with 50S subunits, although they appeared to be normally as-

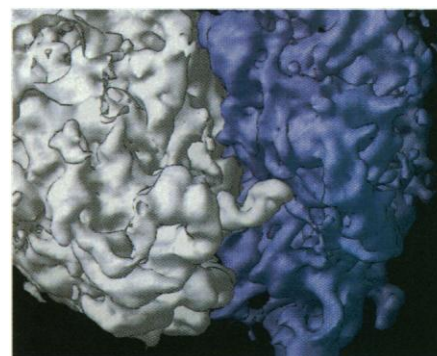


Fig. 1. Electron density from the 7.8 Å crystal structure of the *T. thermophilus* 70S ribosome (4) showing interaction of a discrete RNA feature of the 50S subunit (white) with the bottom of the platform of the 30S subunit (blue). Electron density is contoured at 1.1σ.

Center for Molecular Biology of RNA, Sinsheimer Laboratories, University of California, Santa Cruz, CA 95064, USA.

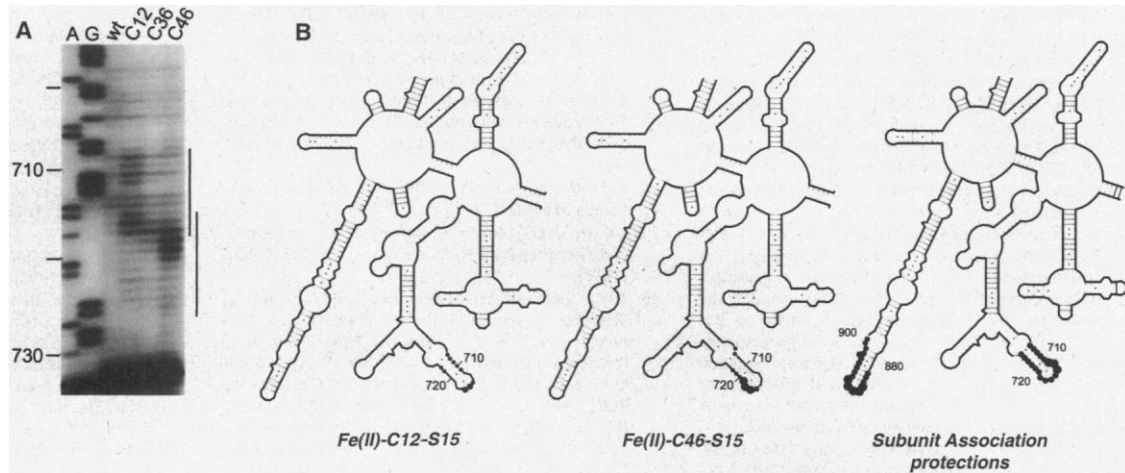
*Present address: Department of Biochemistry, Biophysics, and Molecular Biology, Iowa State University, Ames, IA 50011, USA.

†Present address: Whitehead Institute for Biomedical Research and Massachusetts Institute of Technology, Cambridge, MA 02142, USA.

‡To whom correspondence should be addressed.

REPORTS

Fig. 2. (A) Directed hydroxyl radical cleavage of 23S rRNA in 70S ribosomes containing Fe(II)-derivatized ribosomal protein S15 in reconstituted 30S subunits. Sites of cleavage were localized by primer extension with reverse transcriptase. A and G, sequencing lanes; wt, mock Fe(II)-BABE-treated (cysteine-free) wild-type S15; C12, Fe(II)-C12-S15; C36, Fe(II)-C36-S15; C46, Fe(II)-C46-S15. Vertical lines at the right indicate regions of cleavage. (B) Positions of directed hydroxyl radical cleavage from Fe(II)-C12-S15 and Fe(II)-C46-S15. Nucleotides within this region of 23S rRNA that are protected by subunit association from free hydroxyl radicals (3) are also



shown. Intensities of cleavages are indicated by large, medium, or small solid circles (high through low intensity, according to size).

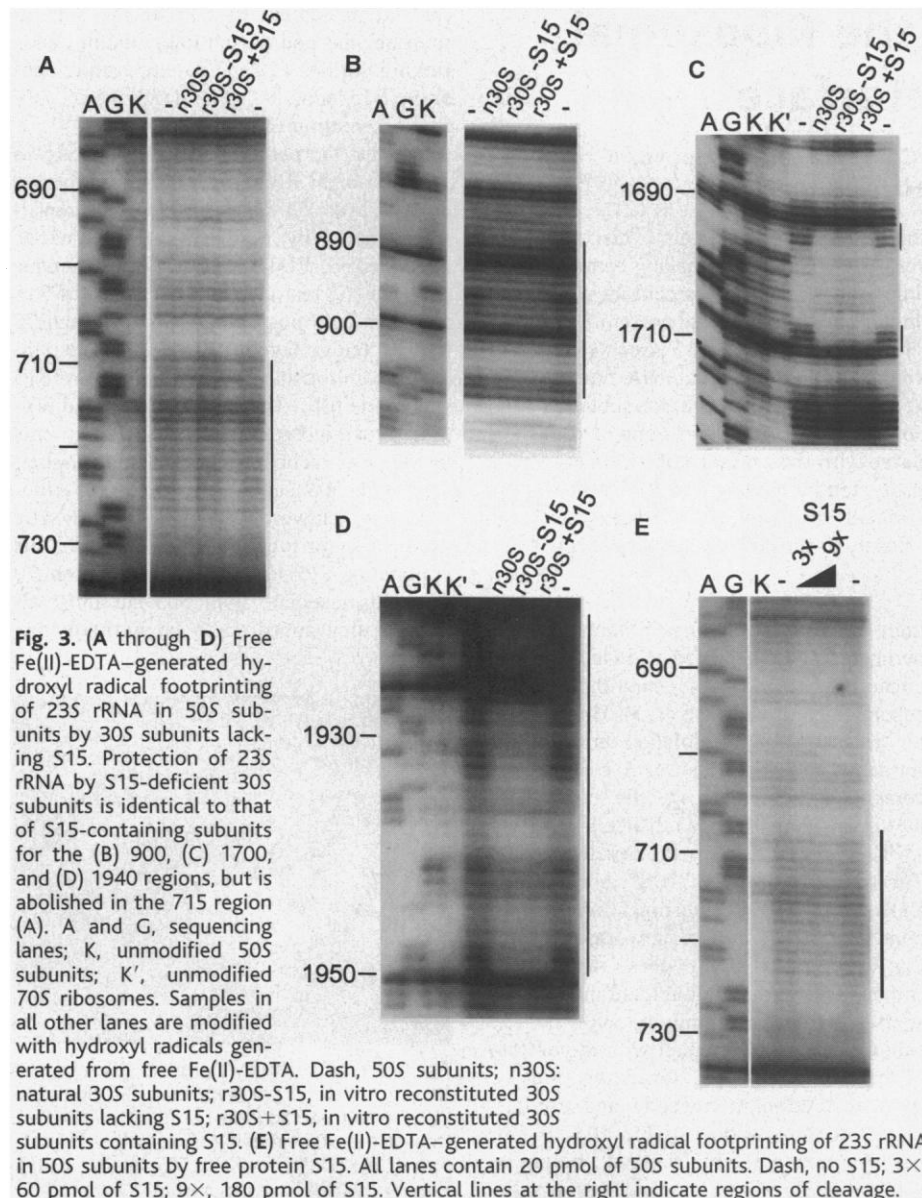


Fig. 3. (A through D) Free Fe(II)-EDTA-generated hydroxyl radical footprinting of 23S rRNA in 50S subunits by 30S subunits lacking S15. Protection of 23S rRNA by S15-deficient 30S subunits is identical to that of S15-containing subunits for the (B) 900, (C) 1700, and (D) 1940 regions, but is abolished in the 715 region (A). A and G, sequencing lanes; K, unmodified 50S subunits; K', unmodified 70S ribosomes. Samples in all other lanes are modified with hydroxyl radicals generated from free Fe(II)-EDTA. Dash, 50S subunits; n30S, natural 30S subunits; r30S-S15, in vitro reconstituted 30S subunits lacking S15; r30S+S15, in vitro reconstituted 30S subunits containing S15. (E) Free Fe(II)-EDTA-generated hydroxyl radical footprinting of 23S rRNA in 50S subunits by free protein S15. All lanes contain 20 pmol of 50S subunits. Dash, no S15; 3×, 60 pmol of S15; 9×, 180 pmol of S15. Vertical lines at the right indicate regions of cleavage.

sembled according to other criteria (12). This result is also consistent with contact between S15 and the 50S subunit. Localized hydroxyl radical production was initiated, and the entire 23S rRNA chain was scanned for sites of rRNA cleavage by primer extension (13). A single region of 23S rRNA, the 715 stem-loop of domain II, was targeted by hydroxyl radicals generated from positions 12 and 46 of S15 (Fig. 2) (14). Overlapping cleavage patterns were observed; nucleotides 707 to 711 and 715 to 717 were targeted by Fe(II)-C12-S15 (Fig. 2), and nucleotides 706 and 707 and 716 to 722 were cleaved by Fe(II)-C46-S15 (Fig. 2). No other cleavage was observed in 23S or 5S rRNA from Fe(II)-S15 (12). Placement of the 715 stem-loop at the subunit interface is supported by hydroxyl radical footprinting studies using free Fe(II)-EDTA (3), which showed that this same region of domain II became protected upon 70S ribosome formation (Fig. 2).

The possibility of direct interaction of S15 with the 715 stem-loop was first tested using footprinting analysis of in vitro reconstituted 30S subunits lacking S15 (15, 16). Solution hydroxyl radical footprinting (17) of the 70S particles showed that the 30S-dependent protection of the 715 region of 23S rRNA was abolished as a result of S15 omission (Fig. 3A), although 30S-dependent footprints were unaffected elsewhere in 23S rRNA (Fig. 3, B through D). Protection of 23S rRNA by 30S subunits reconstituted with S15 was indistinguishable from that of natural 30S subunits (Fig. 3, A through D).

To further test the possible interaction of S15 with the 715 loop, we bound free S15 protein to 50S subunits, and we assessed its interaction with 23S rRNA by hydroxyl radical footprinting (18). The 715 loop of 50S subunits was protected in a concentration-

LINKED CITATIONS

- Page 1 of 2 -



You have printed the following article:

Identification of an RNA-Protein Bridge Spanning the Ribosomal Subunit Interface

Gloria M. Culver; Jamie H. Cate; G. Zh. Yusupova; Marat M. Yusupov; Harry F. Noller
Science, New Series, Vol. 285, No. 5436. (Sep. 24, 1999), pp. 2133-2135.

Stable URL:

<http://links.jstor.org/sici?sici=0036-8075%2819990924%293%3A285%3A5436%3C2133%3AIOARBS%3E2.0.CO%3B2-Y>

This article references the following linked citations:

References and Notes

¹ **Involvement of Bases 787-795 of Escherichia coli 16S Ribosomal RNA in Ribosomal Subunit Association**

William E. Tapprich; Walter E. Hill

Proceedings of the National Academy of Sciences of the United States of America, Vol. 83, No. 3.
(Feb. 1, 1986), pp. 556-560.

Stable URL:

<http://links.jstor.org/sici?sici=0027-8424%2819860201%2983%3A3%3C556%3AIOB7OE%3E2.0.CO%3B2-V>

⁴ **X-Ray Crystal Structures of 70S Ribosome Functional Complexes**

Jamie H. Cate; Marat M. Yusupov; Gulnara Zh. Yusupova; Thomas N. Earnest; Harry F. Noller
Science, New Series, Vol. 285, No. 5436. (Sep. 24, 1999), pp. 2095-2104.

Stable URL:

<http://links.jstor.org/sici?sici=0036-8075%2819990924%293%3A285%3A5436%3C2095%3AXCSO7R%3E2.0.CO%3B2-Y>

⁷ **Directed Hydroxyl Radical Probing of 16S rRNA Using Fe(II) Tethered to Ribosomal Protein S4**

Gabriele M. Heilek; Rosemary Marusak; Claude F. Meares; Harry F. Noller

Proceedings of the National Academy of Sciences of the United States of America, Vol. 92, No. 4.
(Feb. 14, 1995), pp. 1113-1116.

Stable URL:

<http://links.jstor.org/sici?sici=0027-8424%2819950214%2992%3A4%3C1113%3ADHRPO1%3E2.0.CO%3B2-U>

NOTE: The reference numbering from the original has been maintained in this citation list.

LINKED CITATIONS

- Page 2 of 2 -



⁷ **Site-Directed Hydroxyl Radical Probing of the rRNA Neighborhood of Ribosomal Protein S5**

Gabriele M. Heilek; Harry F. Noller

Science, New Series, Vol. 272, No. 5268. (Jun. 14, 1996), pp. 1659-1662.

Stable URL:

<http://links.jstor.org/sici?sici=0036-8075%2819960614%293%3A272%3A5268%3C1659%3ASHRPOT%3E2.0.CO%3B2-G>

⁸ **Transfer of Oxygen from an Artificial Protease to Peptide Carbon During Proteolysis**

Tariq M. Rana; Claude F. Meares

Proceedings of the National Academy of Sciences of the United States of America, Vol. 88, No. 23. (Dec. 1, 1991), pp. 10578-10582.

Stable URL:

<http://links.jstor.org/sici?sici=0027-8424%2819911201%2988%3A23%3C10578%3ATOOFAA%3E2.0.CO%3B2-K>